SCIREA Journal of Geosciences
ISSN: 2995-7206
http://www.scirea.org/journal/Geosciences
April 1, 2026
Volume 10, Issue 1, February 2026
https://doi.org/10.54647/geosciences170373

Subsurface Soil Investigation for Urban Development: Implication on the Greater-Jos Master Plan, North-Central Nigeria

Wazoh, H. N.[1,*] , Daku, S. S.[1], Mancha, P. S.[1] , Christopher, N.[1], Waziri, S. H.[2], & Mallo, S. J.[3]

[1]Department of Geology, University of Jos, Plateau State, Nigeria

[2]Department of Geology, Federal University of Technology, Minna, Niger State, Nigeria

[3]Deparment of Mining Engineering, University of Jos, Plateau State, Nigeria

*Corresponding author's mail – wazohh@unijos.edu.ng Phone NO. +2348131095003

Abstract

The stability of engineering structures fundamentally depends on understanding subsurface conditions, particularly in reclaimed mined-out areas where ground instability persists. This study investigates subsurface soil characteristics within the Greater-Jos Master Plan area to provide critical subsurface data for sustainable urban development. Integrated geological mapping, 75 vertical electrical soundings (VES), and geotechnical analysis of 38 soil samples were conducted. The area is underlain by Jos-Bukuru Complex rocks (predominantly biotite granites) with lateritised Older Basalts. Resistivity values ranged from 29–2802 Ωm for topsoil (0.5–8.8m thick) and 103.20–891.51 Ωm for weathered layers (1.90–46.60m thick), with overburden thickness varying from 1.2–87.9m. Geotechnical analysis revealed low to

medium plasticity (plasticity index 7.4–21.1%), low to medium swelling potential, and variable shear strength parameters (friction angle 12–43°; cohesion 0–41 kN/m²). Based on integrated resistivity and geotechnical characterisation, the study area was delineated into low (2.6%), moderate (63.2%), and high (34.2%) competence zones. Consequently, the resistivity values are seen as strong determinants of the subsurface condition thereby characterising the study area into low, moderate and high competent zones. The geologic/lithologic classification of each layer based on this characterisation has shown that the clayey material encountered is incompetent for engineering purpose. The weathered layer and laterite are rated moderately competent while the fresh granite and compact laterite is rated highly competent. These findings provide essential baseline data for foundation design, land-use planning, and sustainable infrastructure development within the Greater Jos Master Plan area. It is recommended that Foundations should be designed to sit comfortably on competent bedrock or by employing suitable foundation methods such as piling to ensure stability of structures.

Keywords: *Competence; Greater-Jos Master Plan; Mined-out; Subsurface; Urban Development*

1.0 INTRODUCTION

The rapid urbanisation witnessed across developing nations, particularly in sub-Saharan Africa, has intensified the demand for suitable construction land, often forcing development onto marginal or previously disturbed ground. Nowhere is this challenge more pronounced than in areas with complex geological histories, where anthropogenic activities such as mining have significantly altered subsurface conditions. The properties of the subsurface earth materials and the mechanical properties of the overburden will greatly influence the stability and safety of an engineering structural setting (Olayanju et al., 2017). The stability and safety of engineering structures—buildings, roads, bridges, and dams—are intrinsically linked to the geotechnical properties of underlying earth materials, yet site-specific subsurface investigations remain woefully inadequate in many developing regions (Adeyemo & Omosuyi, 2012; Oyeyemi et al., 2020). According to Adeyemo and Omosuyi (2012), the design of the foundation of any engineering structure would require that the depth to subsurface bedrock and geotechnical properties of the soils be properly determined.

The Greater-Jos Master Plan, conceived to guide sustainable urban expansion across Jos North, Jos South, and Jos East Local Government Areas, envisions both shallow and deep foundations for low- and high-rise structures (Government of Plateau State, 2009). However, successful implementation of this ambitious development agenda requires comprehensive understanding of subsurface conditions—knowledge that is currently fragmented and insufficient. This represent a challenge to a safe urban planning for the city, since investigations are seldom carried out before construction. Previous investigations on the Jos-Plateau have documented the engineering properties of lateritic soils (Lar et al., 2011; Wazoh, 2017; Vincent et al., 2020, Wazoh & Mallo, 2021, Daku & Igwe, 2024). But systematic integration of geophysical and geotechnical approaches for site characterisation remains limited. Furthermore, the behaviour of soils derived from granitic and basaltic parent materials in this region, particularly in areas affected by mining disturbances, has received inadequate research attention. Literatures on the engineering properties of soils on the Jos Plateau revealed that soil investigation from an engineering point of view have been greatly overlooked even when these soils are being used as major source of construction and foundation material (Bolarinwa, 2010; Chukwuma, 2010; Lar et al., 2011; Bolarinwa & Ola, 2016; Wazoh, 2017; Okagbue et al., 2018). Except for Government owned projects, study of the behaviour of soils have been neglected by the general public (Ubido et al., 2017; Wazoh & Mallo, 2021). Furthermore, some parts of the land previously subjected to mining activities left the land littered with mine spoils and reclaimed land yet to stabilise (Mallo, 2007; Mallo & Wazoh, 2014). Lack of geophysical investigation is also a contributing factor to these menaces. Oyeyemi et al. (2020) also revealed the lack of adequate information about the near-surface characterisation prior to construction as a contributing factor to incessant building collapse and foundation failures. If adequate information is obtained prior to construction, it will guide in building design, foundation type, settlement rate and sub-soil bearing capacity. The consequences of inadequate subsurface investigation are well-documented in Nigeria's construction industry, where building collapses and infrastructure failures have become alarmingly frequent (Okagbue et al., 2018; Ubido et al., 2017). These failures often stem from preventable causes: foundations bearing on compressible clay layers, differential settlement due to variable overburden thickness, inadequate bearing capacity assessments, and ignorance of problematic soil behaviour. Geophysical methods, particularly electrical resistivity surveying, offer rapid and cost-effective means of delineating subsurface layers and identifying potential problem zones (Olorunfemi et al., 2004; Idornigie et al., 2006). When integrated with conventional geotechnical laboratory testing, these methods provide a

powerful toolkit for comprehensive site characterisation (Olayanju et al., 2017; Ayodele et al., 2017).

For planning, choice of construction techniques and design of structures, surface and subsurface features are necessary (Roy & Bhalla, 2017). Therefore, for proper design of the foundation of civil engineering structures in the implementation of the Greater-Jos Master Plan, subsurface site characterisation will be required to provide subsurface information.

2.0 DESCRIPTION OF THE STUDY AREA

The study area lies within the Greater Jos Master Plan region, encompassing portions of Jos North, Jos South, and Jos East Local Government Areas of Plateau State, North-Central Nigeria (Figure 1). It is geographically constrained by Latitudes 09°48'20" to 09°53'20"N and Longitudes 08°53'54" to 08°57'00"E on Naraguta Sheet 168 NE. The area exhibits a characteristic plateau topography with average elevations exceeding 1000 m above sea level, dominated by undulating plains punctuated by residual granite hills and extensive mine pond complexes resulting from historical tin mining operations (Odunuga & Badru, 2015). The region experiences a tropical continental climate with distinct wet and dry seasons. The natural vegetation corresponds to Guinea savanna type, comprising tall grasses interspersed with drought-deciduous trees and shrubs. However, decades of mining activity, urban expansion, and agricultural intensification have significantly modified the original vegetation cover, creating a mosaic of secondary grassland, cultivated areas, and bare mine spoils.

2.1 Geological Setting

The Jos Plateau forms part of the Younger Granite province of Nigeria, a series of anorogenic ring complexes emplaced during Jurassic times (MacLeod, 1971). The study area lies within the Jos-Bukuru Complex, one of the largest and most economically significant Younger Granite intrusions. The predominant lithologies include various textural and compositional variants of biotite granite, with subordinate occurrences of hornblende-fayalite granite and lateritised Older Basalt (Ejeh & Ugbe, 2010). The Jos-Bukuru granites exhibit considerable petrographic variation, including the Rayfield-Gona biotite granite, Jos biotite granite, Delimi biotite granite, Shen hornblende-fayalite granite, and N'gell biotite granite. These rock types are distinguished on the basis of mode of formation, mineralogy, and texture. The Older Basalts, of Tertiary age, occur as remnant patches now extensively weathered to lateritic clays.

The entire region has been subjected to prolonged weathering and erosion, resulting in thick weathering profiles and extensive laterite development.

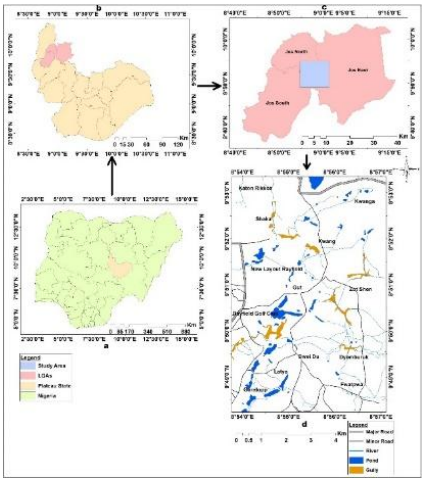

Figure 1 Location Map of the Study Area

Source: Government of Plateau State (2009)

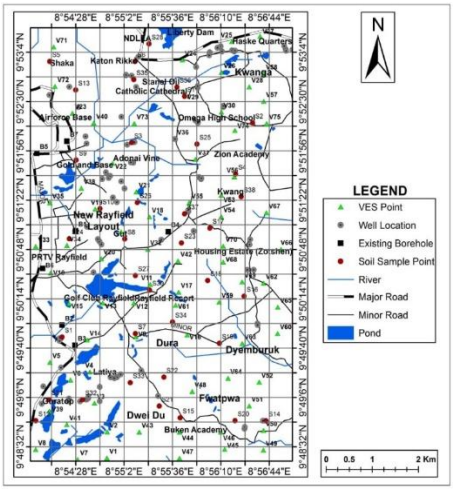

Figure 2 Data Acquisition Map of the Study Area

Source: Modified from National Centre for Remote Sensing [NCRS] (2005)

3.0 MATERIALS AND METHODS

3.1 GEOLOGICAL MAPPING AND GEOPHYSICAL SURVEY

Detailed geological mapping was conducted across the study area where traverses were systematically walked to verify published geology, identify lithological contacts, document weathering profiles, and assess the distribution of mine-affected terrain. A Garmin GPS map 78s Global Positioning System (GPS) receiver was used to record coordinates and elevations of all observation points, sample locations, and VES stations. A thematic engineering geologic map was generated by integrating field observations with SPOT satellite imagery (SPOT, 2001) processed in ILWIS 3.3 GIS environment (ILWIS, 2005).

The Schlumberger vertical electrical resistivity sounding (VES) method of geophysical survey using ABEM Terrameter SAS 1000 model was carried out for determination of earth resistivity for seventy-five locations with electrode separations (AB/2) varying from 1 to 215m and depth penetration of about of 71m. The apparent resistivity values were calculated using the measured resistance in conjunction with the appropriate geometric factor (K) for the electrode configuration and separation as described by (Reynold, 1998). The Computer-

generated curves were compared with corresponding field curves by using a computer program Interprex 1-D sounding version 2006. The software was further used for both computer iteration and modelling. VES results and interpretations as obtained from the model curves were based on the approximate values of resistivity of common earth materials by Milson (2003). From the interpretation of results (layer resistivity values and thicknesses), lithological and geo-electric layers were delineated. Geo-electric sections were constructed along 4 profiles in four directions: SSW-NNE, NE-SW, NW-SE and W–E for correlation of the geo-electric sequence across the study area. The VES points were also correlated with available borehole data. Descriptive statistics (mean, standard deviation, range) were computed for resistivity values, layer thicknesses, depth to bedrock, and elevation using SPSS v.7 (SPSS, 2019) to characterise central tendency and variability of geoelectrical parameters.

3.2 DETERMINATION OF GEOTECHNICAL PROPERTIES

3.2.1 Soil Sampling Procedure

Thirty-eight (38) disturbed and undisturbed soil samples were collected from trial pits excavated to depths of 1.0–3.0 m across representative geological units (Figure 2). Sampling depth was determined by trial pit availability, following standard procedures (Barth & Mason, 1984). Disturbed samples were obtained after clearing surface debris, sealed in polythene bags, and transported to the laboratory. Undisturbed samples were collected by driving thin-walled sampling tubes into cleaned pit faces, sealing ends with wax to preserve in-situ moisture and structure.

3.2.2 Laboratory Analysis

All laboratory tests were conducted in accordance with British Standard 1377 (BSI, 1990; 2000) and BS 772 (BSI, 2011). The Unified Soil Classification System (USCS) was adopted for soil classification.

Particle Sie Distribution - Representative portions (500 g) of oven-dried samples were mechanically sieved through a nested set of sieves (75 mm to 75 μm) for 10–15 minutes. Fractions retained on each sieve were weighed, and percentage passing calculated. Particle size distribution curves were plotted semi-logarithmically.

Atterberg Limits - Liquid limit was determined using the Casagrande percussion cup method. Samples passing the 425 μm sieve were mixed with distilled water, placed in the cup, grooved, and subjected to repeated drops until groove closure. Moisture content corresponding to 25 blows was taken as liquid limit. Plastic limit was determined by rolling soil threads to 3 mm

diameter until crumbling, with moisture content at this point recorded. Plasticity index was calculated as PI = LL - PL. Linear shrinkage was measured by oven-drying soil paste in a standard mould and calculating percentage length reduction.

Compaction Characteristics: Standard Proctor compaction tests were performed using 2.5 kg rammer falling 300 mm, with soil compacted in three layers (25 blows per layer). Maximum dry density (MDD) and optimum moisture content (OMC) were determined from compaction curves.

Shear Strength Parameters: Undisturbed samples were subjected to unconsolidated undrained (UU) triaxial compression tests at confining pressures of 15, 30, and 45 kN/m². Major principal stress at failure (σ_1) was recorded, and Mohr circles constructed. Cohesion (c) and angle of internal friction (φ) were derived from the Mohr-Coulomb failure envelope.

3.3 EVALUATION OF THE SUITABILITY OF SUBSURFACE SOIL

Subsurface competence was evaluated using an integrated approach combining geoelectrical and geotechnical parameters. Topsoil resistivity values at approximately 2 m depth were correlated with geotechnical properties of samples from equivalent depths. Competence classification followed the scheme of Olorunfemi et al. (2004); Idornigie et al. (2006), which relates resistivity ranges to lithological types and engineering competence (Table 1). Spatial distribution of competence zones was mapped by importing resistivity data into GIS, assigning weights to each layer, and generating a composite subsoil competence map using overlay analysis (Olurunfemi et al., 2004; Ofomola, 2018). Plasticity index values from 38 locations were used to validate the competence classification.

Table 1 Rating of Subsoil Competence Using Resistivity Values

Apparent resistivity range (Ωm)	Lithology	Competence rating
<100	Clay	Incompetent
100 – 350	Clayey sand, laterite, weathered granite	Moderately competent
350 – 750	Laterite, weathered granite	Competent

>750	Compact laterite, granite	Highly competent

Source: Idornigie et al. (2006)

4.0 RESULTS AND DISCUSSION

4.1 GEOLOGICAL AND GEO-ELECTRICAL CHARACTERISTICS

The study area is underlain by Jos-Bukuru Complex granites with subordinate lateritised older basalts (Figure 3). Detailed mapping revealed that approximately 20% of the area exposes hard rock outcrops, predominantly as residual hills, boulder fields, and isolated inselbergs. The remaining 80% is covered by varying thicknesses of residual and transported soils derived from in-situ weathering and anthropogenic reworking (Figure 3). Profile thickness varies considerably, controlled by parent rock type, fracture density, topographic position, and mining disturbance.

Geo-electrical Characteristics

A summary of the VES interpretation presented in Table 2 is based on the approximate range of resistivity values of common geologic materials, model curves and the geology of the study area. This gives the layer resistivity and thickness with the inferred lithology of each VES point. The interpretation revealed topsoil, clay, clayey sand, laterite, weathered and partially weathered granite and fresh granite as the subsurface geology of the study area. The H-type curve ($\rho_1 > \rho_2 < \rho_3$) predominated, accounting for 61.33% of soundings, characteristic of weathered crystalline basement terrain with conductive intermediate layer. A-type curves ($\rho_1 < \rho_2 < \rho_3$) constituted 32%, indicating progressively increasing resistivity with depth. K-type curves ($\rho_1 < \rho_2 > \rho_3$) represented 5.33%, while Q-type curves ($\rho_1 > \rho_2 > \rho_3$) comprised only 1.33%. This heterogeneity reflects variable weathering intensity and anthropogenic disturbance.

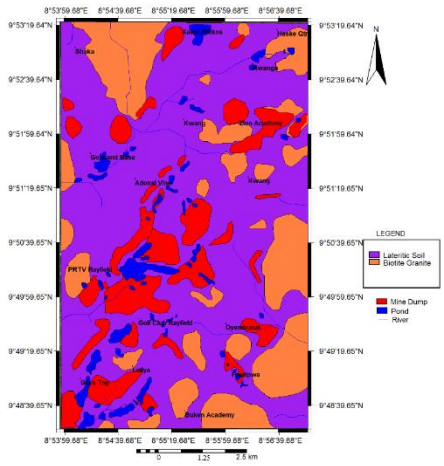

Figure 3 Thematic Engineering Geologic Map of the Study Area Showing Areas Covered by Soils and Pockets of Granites, Mine Dumps and Mine Spoils

Figure 4 Weathering Profile Encountered in the Study Area (N 09° 49' 17.9"; E 08° 54' 24.4", 1308m, Guratopp) (Picture not to scale)

Table 2 Summary of VES Parameters

VES NO.	Resistivity (Ωm) (ρ 1/ ρ 2/ ρ 3…… ρ n)	Layer Thickness (m) h1/ h2/ h3……hn	No. of Layer	Curve Type
V 1	179/1141/98/96	1.5/2.5/46.9	4	K
V 2	230/77/81/126	1.6/13/73	4	H
V 3	891/182/129/12210	8.8/6.9/21.9	4	H
V 4	122/62/29/112	1.6/3.1/15.2	4	H
V 5	292/114/204/776	3.7/11.9/23.1	4	H
V 6	178/52/42/353	2.3/4.1/46.8	4	H
V7	2351/681/416/900/1555	1.2/3.5/16.2/30.2	4	H
V 8	2802/760/508/1358	0.9/2.7/25.2	4	H
V 9	163/772/1010/1641	0.7/16.7/16.1	4	A
V10	585/208/587/499	1.8/15.8/28.7	4	H
V11	953/150/625/5024	1.6/18.2/10.0	4	H

V12	1125/89/305/769/	0.6/7.9/28.2	4	H
V13	759/186/175/1215	2.3/5.9/37.4	4	H
V 14	129/528/358/135	2.5/16.1/22.2	4	K
V 15	279/42/2967/175	2.2/2.9/20.7	4	H
V 16	215/108/326/1554	1.1/9.2/33.9	4	H
V 17	861/104/89/60	0.9/5.4/24.5	4	Q
V 18	462/592/606/737	1.8/5.7/34.0	4	A
V 19	160/275/1017/275	0.9/20.1/31.8	4	A
V 20	371/3005/623/200	4.7/8.9/12.4	4	K
V 21	614/148/2714/14027	1.3/21.9/14.3	4	H
V 22	688/160/690/1544	1.2/17.7/31.7	4	H
V 23	747/372/1552/2711	1.8/3.0/25	4	H
V 24	435/230/668/485	3.7/8.2/36.6	4	H
V 25	562/197/1548/3513	3.5/16.7/14.8	4	H
V26	157/58/205/3172	0.5/9.8/19.4	4	H
V27	243/44/257/2326	0.7/14.6/8.0	4	H
V28	243/44/257/2326	0.7/14.6/8.0	4	H
V29	69/76/362/425	8.4/11.2/28.4	4	A
V30	315/198/895/12946	2.9/18.1/10.1	4	H
V31	628/362/1340/689	3.0/15.6/36.8	4	H
V32	176/32/237/501	4.7/8.3/17	4	H
V33	43/78/60/1518	2.6/4.1/12.4	4	A
V34	179/35/103/459	4.5/6.2/16.2	4	H
V35	1318/493/303.27/1595.8	1.2/4.7/46.6	4	H
V36	439/647/287/199	0.9/13.7/36.5	4	K

V37	195/323/539/510	1.0/10.2/33.8	4	A
V38	102/353/45/246/319	1.8/1.9/5.1/57.8	4	H
V39	395/68/26658/3260	1.9/3.2/48.1	4	H
V40	2210/405.4/3870/1045	3.3/8.9/40.7	4	H
V 41	428/215/647/534	1.6/4.7/27.9	4	H
V 42	714/1347/235/1450	8.2/12.2/36.1	4	H
V 43	2323/539/2577/223	1.5/3.9/42.9	4	H
V 44	533/328/8987/2789	2.4/7.4/34.8	4	H
V 45	2640/432/10090/3266	0.5/11.1/30.9	4	H
V 46	1995/475/8045/3413	0.6/10.3/27.1	4	H
V 47	2269/594/17854/2607.9	0.6/12.9/30.8	4	H
V 48	247/921/18433/955	3.4/1.1/19.9	4	A
V 49	264/756/40782/1309	2.8/0.9/16.5	4	A
V 50	29/153/36462/43459	2.1/1.8/27.7	4	A
V 51	51/1929/309/2993	3.7/14.2/25.6	4	A
V52	119/28703/4321/5643	1.2/2.7/52.2	4	A
V53	890/304/1281/6772	1.5/6.6/8.5	4	H
V54	854/144/1281/9361	4.7/9.9/23.1	4	H
V55	1121/541/3779/87558	1.4/12.2/13.4	4	H
V56	1121/541/3779/87558	1.4/12.2/13.4	4	H
V 57	1131/517/5219/4735	3.9/15.9/34.5	4	H
V 58	965/392/7335/3455	3.2/9.9/31.1	4	H
V 59	2651/612/45464/10231	3.2/13.9/4.2	4	H
V 60	869/11648/33118/13503	6.8/12.9/20.6	4	A
V 61	682/60138/1874/26491	5.9/19.1/28.8	4	A

V 62	2528/519/44393/4124	3.6/8.7/26.9	4	A
V 63	2787/2144/7583/11195	3.5/5.5/8.5	4	A
V 64	2538/2896/45724/3830	3.2/8.2/14.9	4	A
V 65	2102/57600/4461/13846	5.9/10.3/20.2	4	A
V 66	658/559/892/1325	6.7/18.9/24.1	4	A
V67	2152/9433/20932/5251	7.6/7.7/25.4	4	A
V68	126/597/399/9066	3.5/13.3/23.2	4	H
V69	919/424/657/796	3.8/6.9/21.6	4	H
V70	579/116/15276/739	2.5/12.8/21.9	4	H
V 71	78/2821/7956/56117	3.8/9.0/25.5	4	A
V 72	737/3432/54401/2192	2.1/7.6/10.7	4	A
V 73	754/1166/2056/46180	3.9/12.9/7.1	4	A
V 74	851/73/78214/10283	2.9/5.1/37.8	4	A
V 75	917/2239/33410/9090	6.3/2.4/33.1	4	A

Top Layer

Topsoil resistivity values ranged from 29.5 to 2802.3 Ωm (mean = 858.65 Ωm, SD = 790.56 Ωm), with thickness varying between 0.5 and 8.8 m (mean = 2.4 m). Low resistivity values (<100 Ωm) characterised clay-dominated topsoils, occurring principally in areas underlain by deeply weathered N'gell granite and lateritised older basalts (VES 29, 33, 50, 71). Intermediate values (100–350 Ωm) corresponded to clayey sands and sandy clays, while high values (>350 Ωm) indicated lateritic topsoils with significant gravel and nodular components. The topsoil isoresistivity map (Figure 5) revealed distinct spatial patterns: low to moderate resistivity zones occupied Rayfield, Kwang, Guratopp, Katon Rikkos, Kwanga, and Shaka-Gold and Base areas; high resistivity zones (>1000 Ωm) were concentrated at Dwei Du, Shen-Kwang, and Gwarandok, corresponding to areas with thin, gravelly lateritic soils overlying shallow bedrock.

Weathered Layer

The weathered layer (comprising saprolite and partially weathered granite) exhibited resistivity values ranging from 103.2 to 891.5 Ωm (mean = 396.74 Ωm, SD = 361.60 Ωm) and thickness from 1.90 to 46.60 m (mean = 18.7 m). Higher resistivity values (599–891.5 Ωm) occurred on the eastern part (Kwang), southern lower part (Dwei Du), and central area (Rayfield), indicating less intensely weathered, more competent material (Figure 6). Lower resistivity values (<200 Ωm) characterised clay-rich saprolite zones, particularly in areas of deep weathering (Dwei Du, Dura, Gwafan).

Overburden

Total overburden thickness (topsoil + weathered layer) varied dramatically across the study area, ranging from 1.2 to 87.9 m (mean = 24.05 m, SD = 17.25 m). The isopach map (Figure 7) delineated areas of thin overburden (<15 m) around Fwatpwa, Dyemburuk, Shen, and Katon Rikkos, corresponding to bedrock ridges. Thick overburden (>40 m) occurred in areas underlain by Older Basalts (Liberty Dam, Gold and Base) and deeply weathered granites (Dwei Du-Buken Academy), often coinciding with mining-affected terrain.

Bedrock

Fresh granite bedrock resistivity ranged from 1009.7 to 78,214.0 Ωm (mean = 14,344.4 Ωm, SD = 16,797.6 Ωm), reflecting variable fracture density, mineralogy, and degree of incipient weathering. Depth to bedrock varied between 1.2 and 23.3 m (mean = 9.60 m, SD = 5.2 m). The bedrock isoresistivity map (Figure 8) revealed highest resistivities (>10,000 Ωm) at Fwatpwa, Dwei Du, Kwanga, Dyemburuk, Zutshen, and Shaka, indicating competent, massive granite with minimal fracturing. Bedrock relief map (Figure 9) displayed a complex topography of buried ridges and depressions. Prominent bedrock ridges (shallow bedrock) occurred at south-southeast, western, central, and north-northwest sectors (Gwarandok-Katon Rikkos). Deep bedrock depressions (>30 m overburden) occupied eastern, northern, northwestern, and southern parts (Shen-Kwang, Katon Rikkos, Kwang, Shaka), representing palaeo-weathering troughs and valley fills.

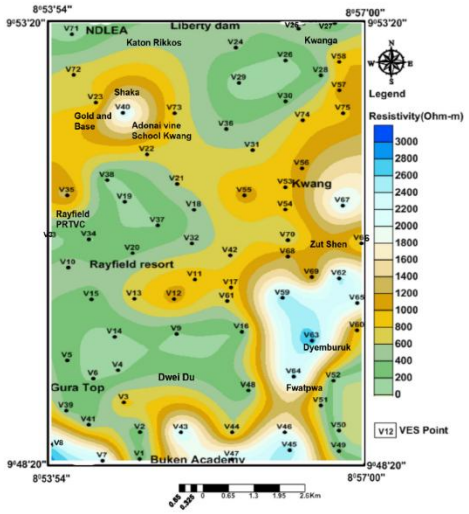

Figure 5 Isoresistivity Map of the Top Layer

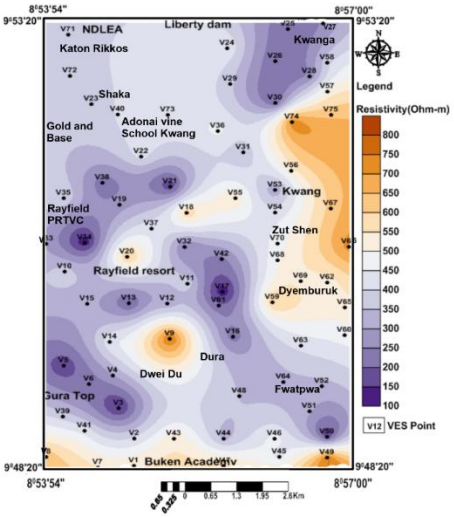

Figure 6 Isoresistivity Map of the Weathered Layer

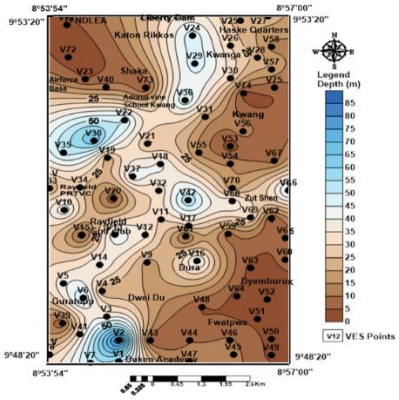

Figure 7 Isopach Map of the Overburden

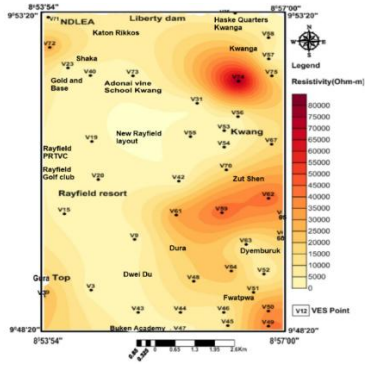

Figure 8 Isoresistivity Map of the Bedrock

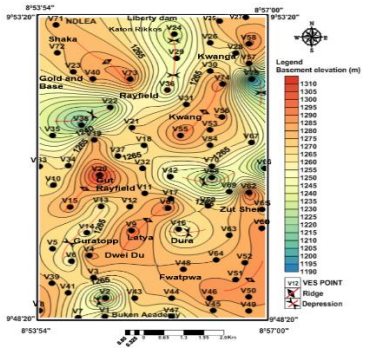

Figure 9 Bedrock Relief Map Showing Depressions and Ridges

Geo-electric Sections

Four geoelectrical sections (W-E, SW-NE, SSW-NNE, NW-SE) illustrated subsurface layer geometry and continuity (Figures 10–13). Four to five geoelectrical layers were typically identified: topsoil (laterite/clayey sand/clay), clay (where present), lateritic layer, weathered granite, and fresh granite. Correlation of VES results with available borehole logs validated

the interpreted lithological sequences. Boreholes intersected three main units: thin lateritic topsoil (0.3–5.0 m), weathered granite/saprolite (24–46 m), and fresh granite. Good correspondence was observed between VES-derived layer boundaries and borehole lithological contacts (Figures 14–15), confirming the reliability of geoelectrical interpretation.

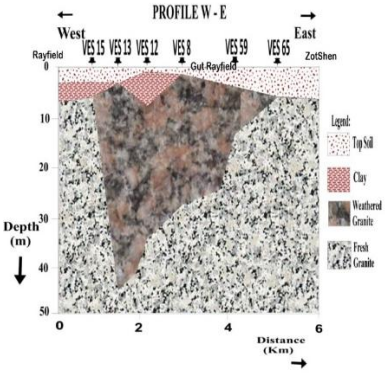

Figure 10 Geo-electric Section (W-E Direction) From Rayfield to Zotshen

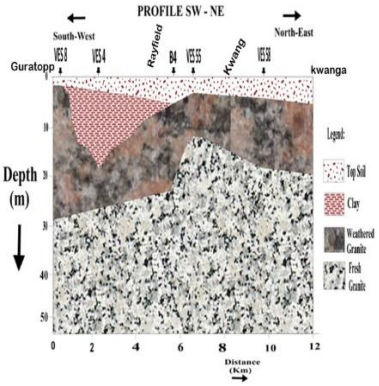

Figure 11 Geo-electric Section (SW - NE Direction) From Guratopp to Kwang

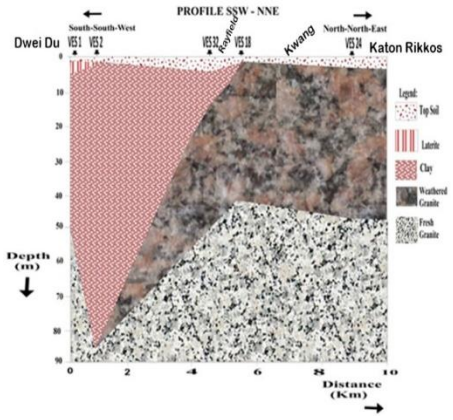

Figure 12 Geo-electric Section (SSW – NNE Direction) From Dwei Du to Katon Rikkos

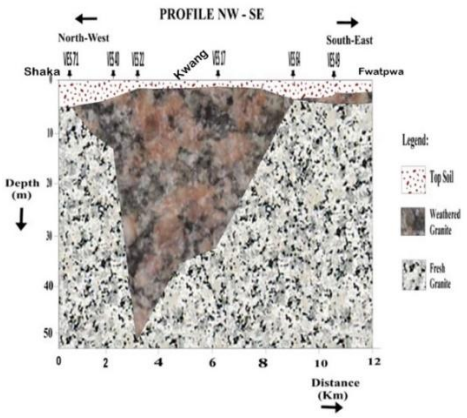

Figure 13 Geo-electric Section (NW SE Direction) From Shaka to Fwatpwa

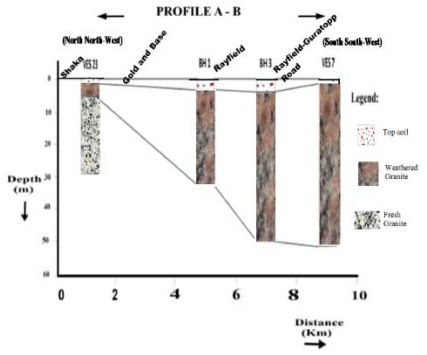

Figure 14 Profile NNW - SSE Showing Corellation of Boreholes with VES Points

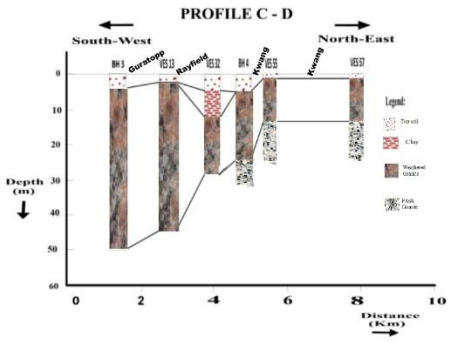

Figure 15 Profile SW - NE Showing Corellation of Boreholes with VES Points

4.2 RESULTS OF GEOTECHNICAL PROPERTIES

Grain size analysis results (Table 3) revealed considerable variation across the study area. Gravel content ranged from 0 to 78.0%, sand from 1.0 to 91.8%, and fines (silt + clay) from 5.4 to 99.0%. Fifty percent of samples exhibited fines content >50%, concentrated in Latya, Kwang, Katon Rikkos, and Dura areas. Samples from Rayfield, Kwang, Gold and Base, and Zot Shen showed moderate fines (20–30%). Based on USCS classification, 78.9% of soils were poorly graded, while 21.1% were well-graded. Liquid limit (LL) ranged from 22.8 to 51.5%, plastic limit (PL) from 9.1 to 42.3%, and plasticity index (PI) from 7.4 to 21.1%. According to Casagrande's plasticity chart, 52.6% of samples plotted in the low plasticity range (CL, ML), 39.5% in medium plasticity (CI, MI), and 7.9% in high plasticity (CH, MH) categories. Higher LL values correlated with increased fines content. Plasticity index values (<25%) placed all soils within low to medium plasticity classification, indicating low to medium swelling potential. Linear shrinkage ranged from 5.7 to 17.9%, with 68.4% of samples exhibiting low to medium shrinkage (<10%), and 31.6% showing medium to high shrinkage (10–18%). Samples from Katon Rikkos and Guratopp displayed higher shrinkage values. Maximum dry density (MDD) ranged from 1.54 to 2.11 kg/m³, with optimum moisture content (OMC) between 8.2 and 23.8%. Granite-derived soils achieved higher MDD (1.75–2.11 kg/m³) with lower OMC (8.2–18.0%), while basalt-derived soils showed lower MDD (1.54–1.72 kg/m³) and higher OMC (18.6–23.8%). Soils with higher fines content generally exhibited lower MDD and higher OMC, though exceptions occurred (Samples 28, 29). Angle of internal friction (φ) ranged from 12° to 43° (mean = 24.8°, SD = 8.7°), while cohesion (c) varied from 0 to 41 kN/m² (mean = 21.3 kN/m², SD = 11.6 kN/m²). Higher friction angles (>30°) characterised well-graded, granular soils from Fwatpwa, Zutshen, and Kwang. Cohesion showed no consistent correlation with fines content. Samples SP31 and SP38 exhibited zero cohesion, indicating purely frictional behavior.

Table 3 Results of Geotechnical Properties of the Soil of the Study Area

Sample No./ Location	Coordinates (degrees) Latitude Longitude	Sieve Analysis			Atterberg Limits					Compaction Characteristics		Strength Parameters	
		Gravel (%0	Sand (%)	Fines (%)	LL (%)	PL (%)	PI (%)	LS (%)	USCS	MDD (kg/m^3)	OMC (%)	ɣ (°)	C_u (KN/m^2)

SP1	9°49' 47.6"; 8°54' 18.5"	24.70	50.70	24.60	39.4	26.8	12.6	9.0	MM	1.82	16.00	25.00	19.00
SP2	9°52' 15.2"; 8°56' 32.3"	7.80	59.30	32.90	45.6	28.0	17.6	9.7	CM	1.80	13.10	15.00	30.00
SP3	9° 52' 01.7"; 8° 55' 7.3"	0.60	75.60	23.80	38.3	20.5	17.8	9.0	CL	1.87	13.10	17.00	33.00
SP4	9° 51'40.0"; 8°56' 20.4"	8.10	76.30	15.60	31.7	21.4	10.3	7.0	CL	1.79	18.90	19.00	31.00
SP5	9° 52' 57.6"; 8° 54' 9.7"	13.10	74.40	12.50	38.6	30.4	8.2	7.6	CL	1.95	14.60	16.00	32.00
SP6	9° 52' 57.6"; 8° 55' 9.7"	0.70	54.90	44.40	47.6	36.7	10.9	9.2	MM	1.60	23.10	20.00	17.00
SP7	9° 49' 50"; 8° 55' 10"	5.50	42.90	51.60	43.8	22.7	21.1	9.1	CM	1.72	21.90	22.00	19.00
SP8	9° 50'55.3"; 8°55' 02.5"	10.20	71.30	18.50	35.1	23.7	11.4	7.4	CL	1.88	16.80	15.00	33.00
SP9	9° 51'49.6"; 8°54' 28.4"	3.70	74.20	22.10	28.4	20.0	8.4	7.1	CL	2.05	11.90	28.00	15.00
SP10	9° 51'16.1"; 8°54' 45.1"	0.70	77.40	21.90	28.0	20.6	7.4	7.0	CL	2.05	11.90	21.00	17.00
SP11	9° 52'33.5"; 8°55' 44.5"	3.77	72.40	23.90	46.9	27.0	19.9	10	CL	1.83	17.00	15.00	32.00
SP12	9° 48' 50"; 8° 54' 00"	13.40	67.80	18.80	36.6	24.1	12.5	9.4	MM	1.76	15.30	23.00	18.00
SP13	9° 52'37.9"; 8°54' 28.0"	32.80	49.20	18.00	54.8	42.3	12.5	10.3	MH	1.76	15.30	19.00	25.00
SP14	9° 48'49."; 8° 56' 41.8"	26.20	56.90	16.90	51.5	NP	NP	NP	NP	1.75	20.00	24.00	15.00
SP15	9° 48'51.9"; 8°55' 41.4"	3.70	64.20	32.10	22.8	9.1	13.7	7.0	CL	1.89	12.00	15.00	28.00
SP16	9° 50'15.8"; 8°56' 26.3"	15.00	55.50	29.50	44.5	40.7	3.8	9.4	MM	1.70	20.90	21.00	18.00

SP17	9° 51' 2.7"; 8° 56' 2.3"	1.70	74.80	23.50	48.2	28.0	20.2	10.0	CM	1.63	22.10	33.00	9.00
SP18	9 49' 43.3"; 8° 56' 9.0"	5.80	83.70	10.50	39.0	27.5	11.5	8.9	MM	2.11	8.20	37.00	9.00
SP19	9° 50' 26.6"; 8 56' 0.8"	19.30	80.10	10.60	37.9	28.5	9.9	7.4	ML	1.69	7.30	27.00	25.00
SP20	9° 48' 50"; 8° 56' 20"	3.30	86.50	10.20	45.8	28.5	17.3	8.5	MM	1.86	15.60	30.00	11.00
SP21	8° 55' 26.7"; 9° 49' 00"	0.50	91.80	7.70	37.9	28	9.9	7.6	ML	2.02	16.90	34.00	15.00
SP22	8° 55' 30"; 9° 49' 20"	4.80	87.10	8.10	33.8	21.9	11.9	7.2	CL	1.99	10.90	37.00	5.00
SP23	8°55' 42.4"; 9°50' 52.5"	6.20	88.40	5.40	37.5	28.5	9.0	7.4	ML	1.82	8.4.00	-	-
SP24	8°54'23.49";9°50' 55.38	15.00	48.00	37.00	41.2	32	9.2	11.1	MM	1.82	16.00	23.00	41.00
SP25	8°55'53.23";9°52'0. 65"	8.00	38.00	54.00	47.8	37.7	10.1	10.9	MM	1.74	18.10	-	-
SP26	8°55'11.31";9°51' 0.37"	25.0	41.00	34.00	46.8	34.7	12.1	10.0	MM	1.87	14.70	-	-
SP27	9° 50' 30"; 8° 55' 10"	13.0	34.00	53.00	51.0	37.2	13.8	10.7	MH	1.89	17.30	30.00	21.00
SP28	9°53'09.68";8°55'19.55"	11.0	37.00	52.00	48.0	36.0	12.0	10.2	MM	1.57	23.80	14.00	28.00
SP29	9°53'34.91";8°54'42.57"	5.00	40.00	55.00	48.2	37.6	10.6	10.0	MM	1.54	22.70	17.00	24.00
SP30	9° 50' 20"; 8° 55' 20"	78.0	13.00	9.00	30.3	22.5	7.8	5.7	ML	1.88	15.800	-	-
SP31	9° 49'04.6"; 8°54' 09.2"	1.00	11.00	88.00	42.6	33.7	8.9	11.4	CM	1.67	18.60	41.00	0.00
SP32	9° 49'04.5"; 8°54' 32.9"	7.00	40.00	53.00	37.5	28.7	8.8	7.1	ML	1.80	15.00	34.00	27.60

SP33	9° 49'16.2"; 8°55' 06.4"	18.00	14.00	68.00	41	30.1	10.9	9.3	ML	1.62	13.50	20.00	34.50
SP34	9° 49' 58"; 8° 55' 36.1"	7.00	27.00	66.00	45.5	35.5	10	10	MM	1.72	18.60	29.00	13.90
SP35	9°52' 45.1"; 8°55' 08.9"	1.00	7.00	92.00	44.2	26.5	17.7	17.9	CM	1.66	16.00	25.00	34.50
SP36	9°52'39.9"; 8° 55' 39.2"	0.00	1.00	99.00	38.0	23.0	15	10.7	CL	1.72	14.50	12.00	20.70
SP37	9°51' 12.5"; 8°55' 44.5"	1.00	27.00	72.00	37.1	28.0	9.1	17.7	ML	1.78	19.40	25.00	27.60
SP38	9°51'24.3"; 8° 56' 24.3"	16.00	28.00	56.00	39.0	28.9	10.1	14.3	ML	1.81	15.70	43.00	0.00

4.3 COMPETENCE EVALUATION FOR SUITABILITY OF ENGINEERING CONSTRUCTION

Integration of topsoil resistivity and plasticity index data enabled spatial delineation of engineering competence zones (Figure 16). Based on the classification scheme (Table 1), the study area comprised of low competence zone (2.6% of area) with resistivity <100 Ωm, clay-dominated lithology, occurring in south-southeastern sector (Fwatpwa-Dyemburuk). The moderate competence zone (63.2% of area) with resistivity 100–750 Ωm, comprising clayey sands, laterites, and weathered granite. The high competence zone (34.2% of area) with resistivity >750 Ωm, representing compact laterite and fresh granite. Validation using plasticity index data showed 60% correlation with resistivity-based classification. Non-expansive behaviour, confirmed by low to medium plasticity indices and linear shrinkage values, further supported the competence assessment.

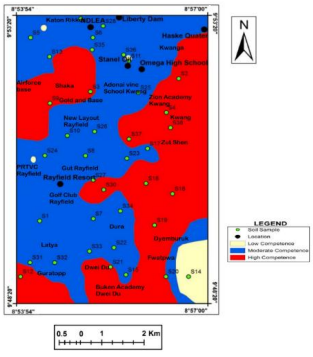

Figure 16 Sub-soil Resistivity Competence Map of Study Area

5.0 DISCUSSION

5.1 Geology Control on Subsurface Conditions

This study confirms that biotite granites, particularly the N'gell and Rayfield Gona variants, are more susceptible to deep weathering than the Jos and Delimi biotite granites, consistent with observations by Ejeh and Ugbe (2010) on fracture-controlled weathering in Younger Granite terrains. The preferential weathering of N'gell granite areas explains the thick overburden (>50 m) encountered in Dwei Du and Buken Academy sectors, which coincides with intensive historical mining activity. The Jos-Bukuru Complex granites exhibit considerable textural and compositional variation that fundamentally influences weathering patterns and resultant soil properties. The lateritised Older Basalts, though occupying limited area, produce distinct soil characteristics—higher fines content, lower density, and higher moisture retention—that contrast with granite-derived soils. This aligns with Obermeier and Langer's (1986); Adeola & Oyebola (2016); Adeola & Dada (2017) observation that mafic rocks weather to clay-rich soils with different engineering behaviour than felsic-derived soils. However, the basalt-derived soils in this study remain in the kaolinitic weathering stage rather than progressing to montmorillonitic clays, explaining their moderate rather than high swelling potential. Weathering profiles observed in trial pits and inferred from VES data reflect progressive decomposition from fresh rock through saprolite to residual soil, with systematic changes in texture, mineralogy, and engineering properties. The predominance of H-type geoelectrical curves (61.33%) typifies this weathering profile in crystalline basement environments (Reinhard, 2006; Idornigie & Olorunfemi, 1992), where conductive clay-rich intermediate layers develop between resistive topsoil and resistive bedrock. The occurrence of A-type (32%) and K-type (5.33%) curves indicates local variations in weathering intensity and leaching regimes, likely influenced by topographic position, drainage conditions, and mining disturbance.

5.2 Geo-electrical Characteristics

The wide range of topsoil resistivity values (29–2802 Ωm) reflects the heterogeneous nature of surface materials, comprising mixtures of residual laterite, transported colluvium, and mining spoils. This heterogeneity, uncommon in undisturbed basement terrains, results from anthropogenic reworking and has significant implications for foundation design, as adjacent building plots may encounter entirely different subsurface conditions. Weathered layer resistivity (103–891 Ωm) and thickness (1.9–46.6 m) variations indicate differential

weathering intensity controlled by fracture density, mineralogical susceptibility, and groundwater conditions. Higher resistivity weathered zones (>500 Ωm) in Kwang, Dwei Du, and Rayfield suggest less intense alteration with preserved rock fabric, offering better foundation conditions than low-resistivity clay-rich saprolite zones. The bedrock relief map (Figure 9) reveals a complex buried topography with ridges and depressions, similar to palaeo-weathering surfaces documented elsewhere in basement terrains (Olorunfemi & Okhue, 1992; Adagunodo et al., 2018). Bedrock depressions, often filled with thick sequences of weathered material and clay, pose particular engineering challenges: (1) differential settlement potential where structures straddle depression margins; (2) thicker compressible layers; and (3) possible groundwater concentration. Conversely, bedrock ridges offer shallow foundations bearing directly on or near competent rock.

5.3 Geotechnical Property and Engineering Implications

The predominance of poorly-graded soils (78.9%) reflects the immature nature of these residual materials and the limited transport history. The high fines content (>50%) in 50% of samples, particularly in Latya, Kwang, Katon Rikkos, and Dura, indicates advanced weathering states where feldspars have completely altered to clay minerals. This finding corroborates earlier work by Lar et al. (2011) and Wazoh (2017) on Jos Plateau soils, though the current study documents greater spatial variability. The engineering significance of high fines content is twofold. First, finer soils are more susceptible to erosion and surface water damage, requiring careful drainage design (Amagu et al., 2018). Second, soils with fines content between 20–30% (Samples 1, 3, 9, 10, 11, 16, 17) satisfy Daniel's (1993) criterion for effective hydraulic barriers, suggesting potential suitability as landfill liner materials after appropriate compaction. Liquid limit values (22.8–51.5%) classify these soils as low to intermediate compressibility according to ASTM (2006) standards. Crucially, all plasticity index values (<25%) fall below the 25% upper limit recommended for sub-base and sub-grade materials (Adeyemi, 2002; Olayanju, 2011), indicating general suitability for foundation construction. The low to medium plasticity (PI 7.4–21.1%) and corresponding low to medium swelling potential contrast sharply with truly expansive soils documented elsewhere (Azam et al., 2013; Christodoulias, 2015), which exhibit PI values >30% and LL >60%. This non-expansive behaviour, consistent with kaolinitic clay mineralogy (Alhassan et al., 2014; Ural, 2018), suggests that foundation problems in the study area will likely arise from differential settlement, inadequate bearing capacity, or poor drainage rather

than shrink-swell phenomena. However, localised higher linear shrinkage values (up to 17.9%) in Katon Rikkos and Guratopp warrant site-specific investigation before construction.

Maximum dry density values (1.54–2.11 kg/m³) compare favourably with those reported for residual tropical soils elsewhere (Osinubi et al., 2012; Odunfa et al., 2018). The higher MDD and lower OMC of granite-derived soils indicate better compaction response and greater strength potential than basalt-derived soils. This differential behaviour must inform material selection for engineered fills and pavement construction. The inverse relationship between fines content and MDD, though statistically weak in this dataset, suggests that soils with excessive fines (>50%) will require more rigorous compaction effort or modification to achieve required densities. Areas with very high fines (Samples 28, 29) exhibited elevated OMC (>22%), indicating greater sensitivity to moisture conditions during construction. The wide range of friction angles (12–43°) and cohesion values (0–41 kN/m²) reflects the diverse soil types and weathering states encountered. Higher friction angles (>30°) characterise granular, well-graded soils from Fwatpwa, Zutshen, and Kwang, which will provide better bearing capacity for shallow foundations. The absence of correlation between cohesion and fines content, contrary to Dafalla's (2013) observations, suggests that cementation by iron oxides and preserved relict fabric may contribute to cohesive strength independently of clay content. Zero cohesion values in Samples 31 and 38 indicate purely frictional behaviour, requiring careful foundation depth and width design to mobilize adequate bearing resistance. These shear parameters, while not fundamental soil properties, enable preliminary bearing capacity estimates when substituted into appropriate formulae (Terzaghi, 1943; Craig, 2004).

The integration of geoelectrical and geotechnical data provides a robust framework for engineering zonation, overcoming the limitations of either method used alone. The 60% correlation between resistivity-based competence classification and plasticity index validation is encouraging, suggesting that VES can reliably extrapolate point-specific geotechnical data across larger areas. Low competence zones (<100 Ωm) in the south-southeastern sector (Fwatpwa-Dyemburuk). These areas require either avoidance for heavy structures or specialised foundation designs (piles to bedrock, ground improvement, or raft foundations). The predominance of moderate competence zones (63.2%) indicates that most of the study area can support conventional shallow foundations for low-rise structures, provided standard geotechnical investigation precedes individual developments. High competence zones (34.2%) in Fwatpwa, Dwei Du, Kwanga, Dyemburuk, Zutshen, and Shaka offer optimal sites for high-rise buildings, industrial facilities, and critical infrastructure.

CONCLUSION

The depth to competent bedrock and overburden thickness has strong influence on foundation stability. Consequently, the resistivity values are seen as strong determinants of the subsurface condition thereby characterising the study area into low, moderate and high competent zones. The geologic/lithologic classification of each layer based on this characterisation has shown that the clayey material encountered is incompetent for engineering purpose. The weathered layer and laterite are rated moderately competent while the fresh granite and compact laterite is rated highly competent. The geotechnical properties are significantly influenced by the parent rock mineralogy and its degree of weathering as indicated by the variation in the physical properties of the soils. Though the parent rock plays a significant role in engineering behaviour of soils, but to a larger extent the degree of weathering and reworking of the soils by mining activity has played a greater significance in the studied soils. The Greater Jos Master Plan envisions diverse urban development including residential neighborhoods (low-rise), commercial centers (mid-rise), and institutional facilities (variable heights). The subsurface characterisation presented here directly informs several aspects of plan implementation. Areas underlain by high competence materials (34.2%) can accommodate deep foundations for high-rise structures. Moderate competence zones (63.2%) require site-specific bearing capacity analysis; shallow foundations may suffice for light structures, while heavier buildings may need reinforced shallow foundations or piles. Low competence zones (2.6%) demand either avoidance or engineered ground improvement (dynamic compaction, stone columns, deep soil mixing).

ACKNOWLEDGEMENT

The authors acknowledge the Plateau State Government for providing the Greater Jos Master Plan documents and the National Centre for Remote Sensing for providing satellite imagery. Appreciation is extended to Dr. Yusuf N. Solomon of the University of Jos for his guide in the interpretation of the geophysical data.

REFERENCES

[1] Adagunodo, T. A, Akinoloye, M. K, Sunmonu, L. A, Alzebeokhai, A. P., Oyeyemi, K. D., & Abiodunrin, F. O. (2018). Groundwater exploration in Aaba residential area of Akure, Nigeria. *Frontier Earth Science, 6*(66), 1–12.

[2] Adeola, A. J., & Oyebola, A. M. (2016). Mineralogy and geochemistry of the weathering profiles above the basement rocks in Idi-Ayunre and Akure districts, southwestern Nigeria. *Journal of Geography and Geology*, *8*(12), 15–29. doi.org/10.5539/jgg.v8n2p15

[3] Adeola, A. J., & Dada, R. G. (2017). Mineralogy and geochemical trends in lateritic weathering profiles on basement rocks in Awa-Oru Ijebu and its environ, southwestern Nigeria. *Global Journal of Geological Sciences, 15*, 1–11. doi.org/10.4314/gigs.visi.1.1

[4] Adeyemi, G. O. (2002). Geotechnical properties of lateritic soil developed over quartz schist in Ishara area Southwestern Nigeria. J*ournal of Mining and Geology*, *38*(1**),** 65–69.

[5] Adeyemi, G. O., & Oyediran, A. I. (2004). *Subsoil geotechnical investigations of five proposed building sites at the Mini Campus of the Adekunle Ajasin University* (Tech. Rep.). Akungba Akoko, Ondo State: Adekunle Univeristy.

[6] Adeyemo, I. A., & Omosuyi, O. G. (2012). Hydrogeologic, electrical and electromagnetic measurements for geotechnical characterization of foundation beds at Afunbiowo, near Akure, Southwestern Nigeria. *International Journal of Science and Technology*, *5*(20), 17–22.

[7] Alhassan, M., Mustapha, A. M., & Mesaiyete, E. (2014). Influence of clay mineralogy on plasticity of lateritic soils. *Journal of Mechanical and Civil Engineering*, *11*(93),13–21. doi.org/10.9790/1684-11341821

[8] Amagu, A. *C.*, Eze, S. N., Jun-ichi, K., & Nweke, M. O. (2018). Geological and geotechnical evaluation of gully erosion at Nguza Edda, Afikpo Sub-basin, Southeastern Nigeria. *Journal of Environment and Earth Science*, *8*(12), 148-158. Retrieved May 10, 2019, from www.iiste.org

[9] American Society for Testing and Materials, ASTM-D2487. (2006). *Standard practice for classification of soils for engineering purposes.* West Conshohocken: Author. doi.org/10.1520/D2487-00

[10] Ayodele, M. O., Omoirabor, O., & Adiela, U. P. (2017). An investigation of the relationship between electrical resistiivty (Wenner and Schlumberger arrays) and geotechnical parameters in foundation investigation in Basement Complex area of Iloko, Osun state, Nigeria. *International Journal of Scientific Engineering and Science*, *1*(5), 18–23.

[11] Azam, S., Ito, M., & Chowdhury, R. (2013). Engineering properties of an expansive soil. *Proceedings of the 18th International Conference on Soil mechanics and Geotechnical Engineering,* Paris, 199–202. Retrieved June 22, 2019, from https//www.geoengineering.org/index.php/publications/online-library?

[12] Barth, D. S., & Mason, B. J. (1984). *Soil Sampling quality assurance user's guide* (Tech. Rep. No. PB-84-18621). Nevada University, Las Vegas.

[13] Bolarinwa, A. (2010). Geotechnical properties of major problem soils of Nigeria. Retrieved September 20, 2013, from http://engrdemol.hubpages.com/hub/geotechnical-properties-of-Nigerian-soils.

[14] Bolarinwa, A., & Ola, S. A. (2016). A review of the major problem soils in Nigeria. *FUOYE Journal of Engineering and Technology,* 1 (1), 20–25. doi:10.4672/fuoyejet.v1i1.20

[15] British Standards Institute. (1990). *BS 1377-1: Methods of tests for soils for civil engineering purposes.* Milton Keynes.

[16] British Standard Institute. (2000). *BS 1377-2: Methods of tests for soils for civil engineering purposes*. Milton Keynes.

[17] British Standard Institute. (2011). *BS 772-1: Methods of tests for masonry units' determination of compressive strength*. Milton Keynes.

[18] Casagrande, A. (1932). Research on the Atterberg Limits of soils, *Public Roads*, *13*(8), 121–36.

[19] Christodoulias, J. (2015). Engineering properties and shrinkage limit of swelling soils in Greece. *Journal of Earth Science and Climate Change*, *6*(5), 1–6. doi.org/10.4172/2157-7617.1000279

[20] Chuwkuma, R. C. (2010). *Geotechnical properties of reclaimed mine out land sites: a case study of Jos and environs, Sheet 168NE and SE*. Unpublished master's thesis, University of Jos, Jos.

[21] Craig, R. F. (2004). *Craig's Soil mechanics* (7th ed.). London: Spon Press.

[22] Dafalla, A. M. (2013). Effects of clay and moisture content on direct shear tests for clay-sand mixtures. *Advances in Materials Science and Engineering*. *2013*, 1–8. doi.org/10.1155/2013/562726

[23] Daku, S. S., & Igwe, (2024). Characterization of mine spoils for the reclamation of degraded lands of the Jos-Bukuru tin field, central Nigeria. *Journal of Nigeria Society of Physical Sciences, 6*, 1 – 14. doi:10.46481/jnsps.2024.1921

[24] Daniel, D. E. (1993). Clay liners. In D.E. Daniel (Ed.), *Geotechnical practice for waste disposal* (pp.131–163). London: Chapman and Hall.

[25] Ejeh, O. I., & Ugbe, C. F. (2010). Fracture systems in the Younger Granite rocks around Fobur, Northern Nigeria: Product of residual stress? *Global Journal of Geological Sciences*, *8*(1), 57–64.

[26] Government of Plateau State. (2009). *Greater Jos Master Plan.* Jos.

[27] Idornigie, A. I., & Olorunfemi, M. O. (1992). A Geoelectric mapping of the basement structure of the South-Central part of Bida Basin and its hydrogeophysical implications. *Journal of Mining and Geology*, *28*(1), 93–103.

[28] Idornigie, A. I, Olorunfemi, M. O., & Omitogun, A. A. (2006). Electrical resistivity determination of subsurface layers, subsoil competence and soil corrosivity at an engineering site location in Akungba-Akoko, Southwestern Nigeria. *Ife Journal of Science, 8*(2), 159–177.

[29] Integrated Land and Water Information System (ILWIS) -3.3. (2005). -*Remote sensing and GIS Software*. Netherlands: Faculty of Geo-information and Earth Observation (ITC).

[30] Interpex Limited. (2002). Resistivity modeling software- IXID 2.06. Colorado, USA.

[31] Lar, U. A., Wazoh, H. N., Mallo, S. J., & Chup, A. S. (2011). Geotechnical characterization of lateritics soils in Jos and Environs. *Nigerian Mining Journal*, *9*(1), 7–17.

[32] Mallo, S.J. (2007). *Minerals and Mining on the Jos Plateau. Jos*: ACON Publishers.

[33] Mallo, S. J., & Wazoh, H. N. (2014). Reclamation of abandoned mined-out areas of Bukuru- Rayfield. *IOSR Journal of Environmental Science, Toxicology and Food Technology*, *8*(2), 25–34.

[34] MacLeod, W. N (1971). The Jos-Bukuru Complex. *Geological Survey of Nigeria*, *Bulletin, 2*(32), 67–84.

[35] Milson, J. (2003). *Field geophysics, the field guide series.* London: John Willey and Sons Limited.

[36] National Centre for Remote Sensing [NCRS]. (2005). *Drainage Map*. Nigeria.

[37] Nigeria Geological Survey Agency. (2012). *Geological Map*. Nigeria.

[38] Obermeier, S. F., & Langer, W. H (1986). *Relationship between geology and engineering characteristics of soils and weathered rocks of Fairfax County and Vicinity, Virginia*. (Tech. Rep. No. 1344). U. S. Geological Survey. doi.org/10.3133/pp1344

[39] Odunfa, S. O., Owolabi, A. O., Aiyedun, P. O., & Sadiq, Q. M. (2018). Geotechnical assessment of pavement failures along Lagos-Ibadan express way. *FUOYE Journal of Engineering and Technology*, *3*(2), 114–117.

[40] Odunuga, S., & Badru, G. (2015). Landcover Change, land surface temperature, surface albedo and topography in the Plateau Region of North-Central Nigeria. *Land, 4*(2), 300 – 324.

[41] Ofomola, M. O., Iserhien-Emekeme, R. E., Okocha, I. O., & Adeoye, T. O. (2018). Evaluation of subsoil competence for foundation studies at site III of the Delta state University, Nigeria. *Journal of Geophysics and Engineering*, *15*(3), 638-657. doi:10.3390/land4020300.

[42] Okagbue, H. I., Iroham, C. O., Peter, N. J., Owolabi, J. D., Adamu, P. I., & Opanya, A. A. (2018). Systematic review of building failure and collapse in Nigeria. *International Journal of Civil Enginering and Technology, 9*(10), 1391–1401.

[43] Olayanju, G. M. (2011). Engineering geophysical investigation of a flood zone: A case study of Alaba Layout, Akure, southwestern. *Nigeria Journal of Geology and Mining Resource, 3*(8**)**, 193–200.

[44] Olorunfemi, M.O., & Okhue, E. J. (1992). Hydrogeologic and geologic significance of geo-elelctric survey at Ile-Ife. *Nigerian Journal of Mining Geology, 28*(2), 221–229.

[45] Olorunfemi, M. O., Idoringie, A. I., Coker, A. T. A., & Babadiya, G. E. (2004). The application of the electrical resistivity method in foundation failure investigation. *Global Journal of Geological sciences, 2*, 39–51.

[46] Osinubi, K. J., Eberemu, A. O., Bello, A. O., & Adzegah, A. (2012). Effect of fines content on the engineering properties of reconstituted lateritic soils in waste contaminant application. *Nigerian Journal of Technology*, *3*(3), 277–287.

[47] Oyeyemi, K. D., Olofinnade, O. M., Aizebeokhai, A. P., A. P., Sanuade, O. A. Oladunjoye, M. A., Ede, A. N.,… Ayara, W. A. (2020). Geoengineering site characterization for foundation integrity assessment. *Congent Engineering*, *7*(1), 1–16. doi.org/10.1080/23311916.2020.111684

[48] Reinhard, K. (2006). *Groundwater geophysics, a tool for hydrogeology text book.* Berlin, Heideberg, New York: Springer international publishing.

[49] Reynolds, J. M. (1998). *An introduction to applied and environmental geophysics*. New York, NY: John Willey and Sons LTD.

[50] Satelite Pour L'Observation De La Terre [SPOT]. (2001). *Satellite Imagery.* Toulouse, France: CNES.

[51] Statistical Package for the Social Sciences (SPSS). (2019). Version 7.

[52] Ubido, E. O., Igwe, O., Ukah, B. U., & Idris, I. G. (2017). The implication of subsoil geology in foundation failure using geotechnical methods: a case study of Lagos southwestern Nigeria. *International Journal of Advanced Research & Publications, 1*(5), 165 – 174.

[53] Ural, N. (2018). The importance of clay in geotechnical engineering: current topics in the utilization of clay in industrial and medical application. *Intech Open,* 8–102. doi.org/10.5772/intechopen.75817

[54] Vincent, E., Dominic, P., & Kure, M. M. (2020). Assessment of geotechnical parameters of lateritc soil of Jos and environs, for civil engineering constructions North central part of Nigeria. *Nigerian Annals of Pure and Applied Science*, *3*(3), 222–239.

[55] Wazoh, H. N. (2017). Compaction behaviour and classification properties of soils of Kwang/Shen, Jos-Plateau, North-central Nigeria. *Journal of Multidisciplinary Engineering Science Studies*, *3*(2), 1405–1408.

[56] Wazoh, H. N., & Mallo, S. J. (2021). Implications of the engineering geological properties of soils in the implementation of the Greater Jos Master Plan, North Central Nigeria. *European Journal of Engineering and Technology Research*, *6*(5), 118–128.